Supporting Information

Structural Regulation of $PdCu_2$ Nanoparticles and Their Electrocatalytic Performance for Ethanol Oxidation

Jing Xue, Guangting Han, Wanneng Ye, Yutao Sang, Hongliang Li, Peizhi Guo and X. S. Zhao*

Institute of Materials for Energy and Environment, State Key Laboratory Breeding Base of New Fiber Materials and Modern Textile, School of Materials Science and Engineering, Qingdao University, Qingdao 266071 PR China

*E-mail: pzguo@qdu.edu.cn; qduguo@163.com; Tel: +86 532 85953982

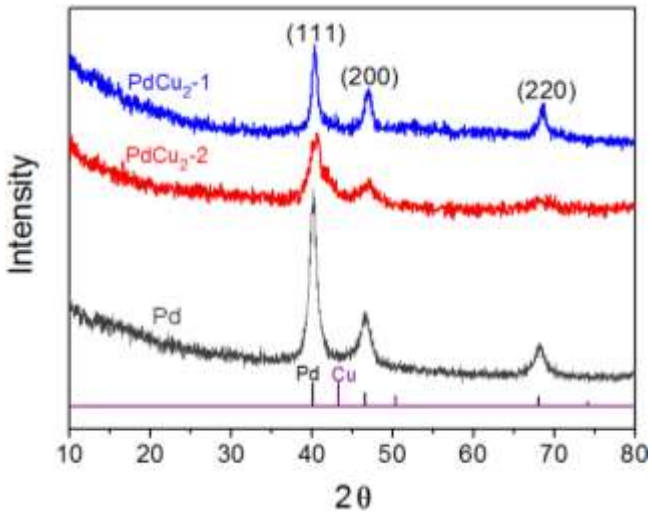

Figure S1. XRD patterns of $PdCu_2$-1, $PdCu_2$-2 and Pd NPs as well as the standard spectra of Pd (JCPDS No. 46-1043) and Cu (JCPDS No. 04-0836).

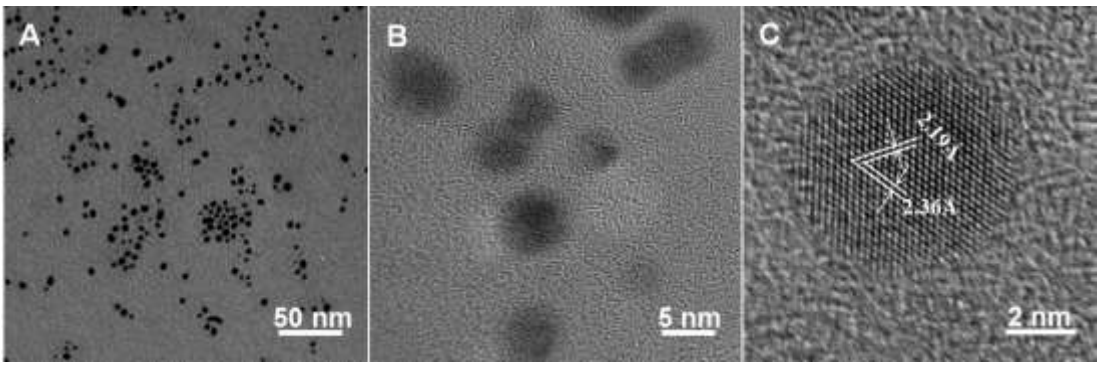

Figure S2. TEM (A, B) and HRTEM (C) images of Pd NPs prepared during the same process as $PdCu_2$-1 without Cu precursors.

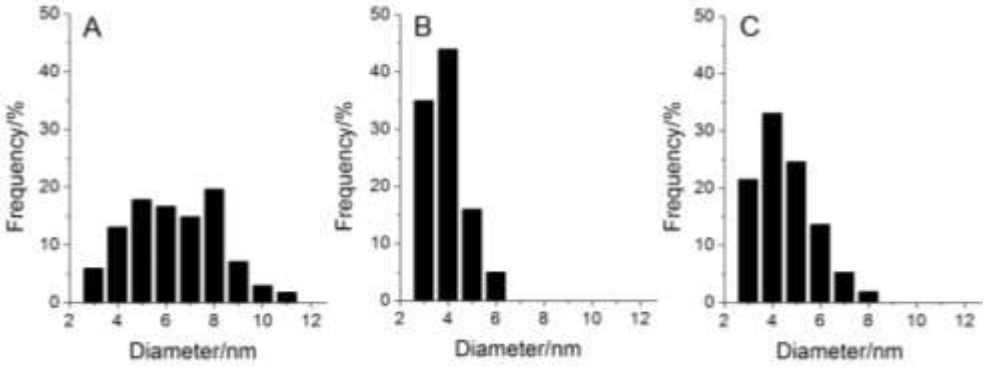

Figure S3. The particle size distribution patterns of $PdCu_2$-1 (A), $PdCu_2$-2 (B) and Pd (C) NPs; each pattern calculated from about 200 particles.

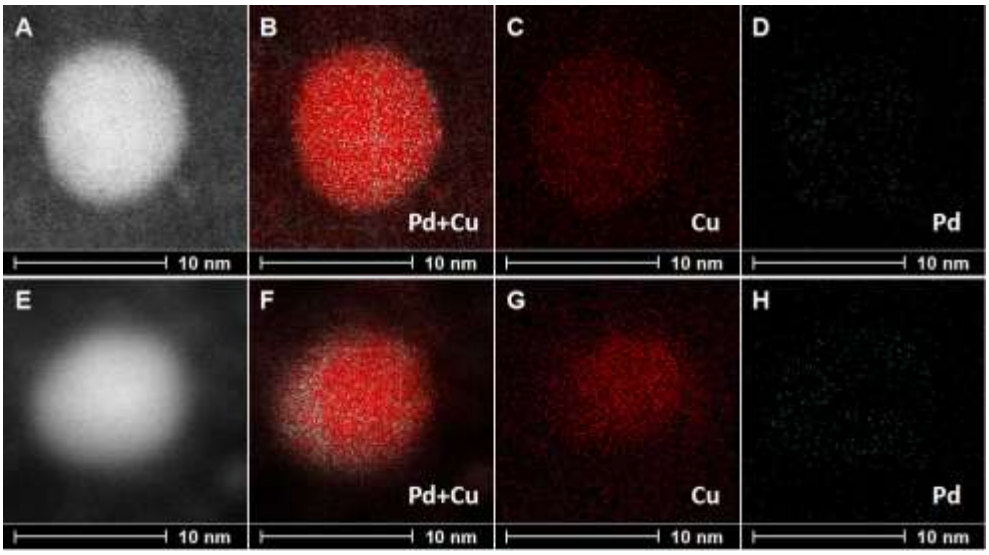

Figure S4. HAADF-STEM images and elemental mappings for single $PdCu_2$-1 (A-D) and $PdCu_2$-2 (E-H) nanoparticle.

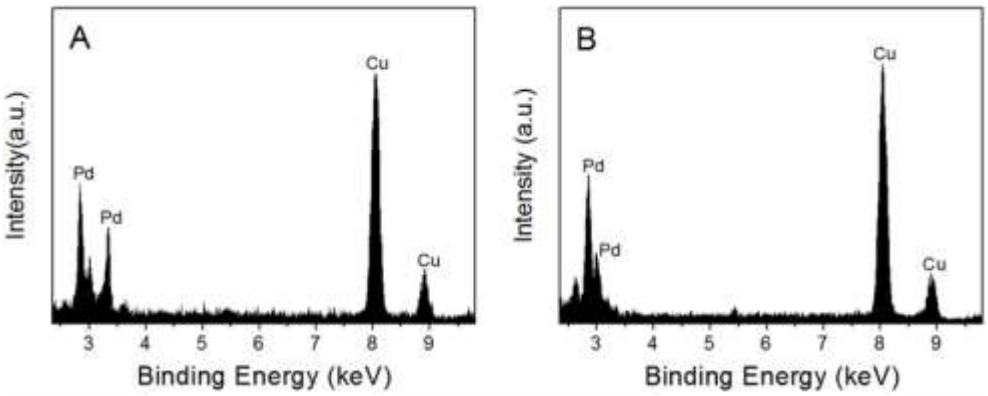

Figure S5. The EDX spectra of $PdCu_2$-1 (A) and $PdCu_2$-2 (B).

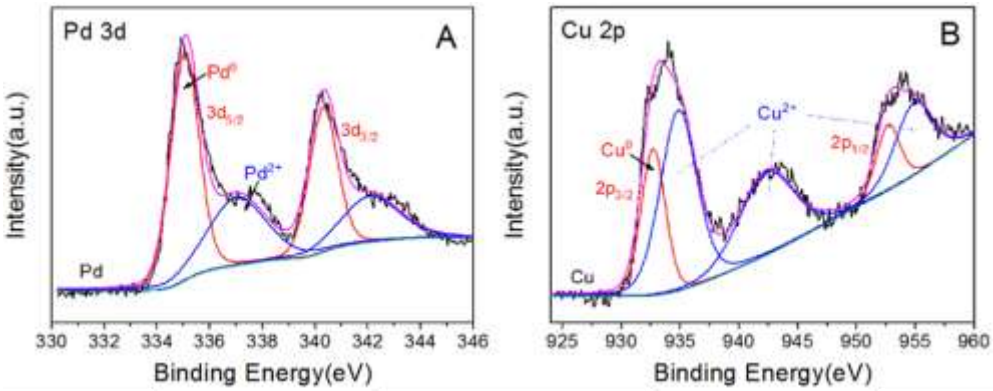

Figure S6. High-resolution XPS spectra of Pd 3d for pure Pd (A) and Cu 2p regions for pure Cu (B).

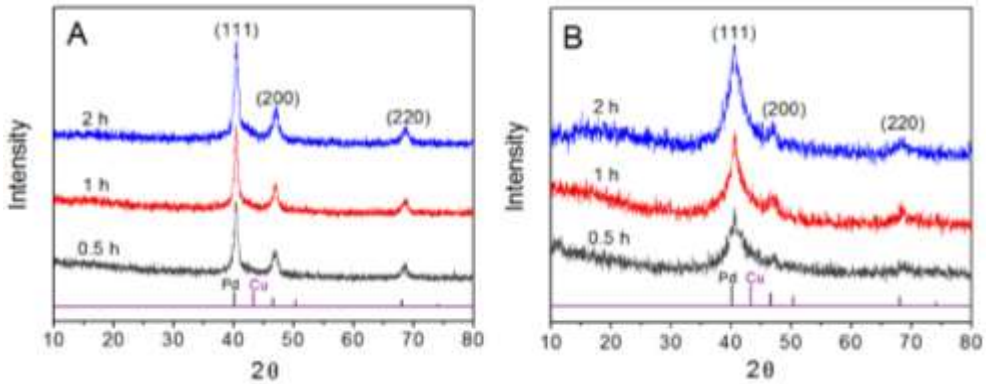

Figure S7. XRD patterns of intermediary products at different intervals during the formation process of $PdCu_2$-1 (A) and $PdCu_2$-2 (B).

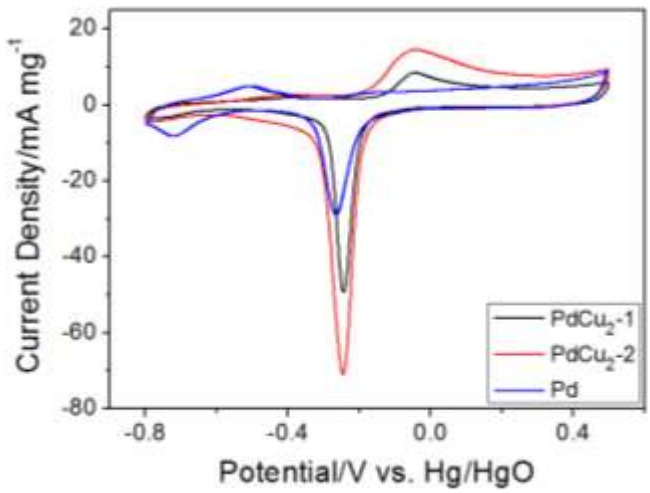

Figure S8. CVs of $PdCu_2$-1, $PdCu_2$-2 and Pd NPs in 1 M KOH at a scanning rate of 20 mV s^{-1}.

Catalysts	ECSA (m^2 g^{-1})		
	$\frac{Q_{H_{des}}}{210\mu C\ cm^{-2}}$	$\frac{Q_{Cu_{upd}}}{420\mu C\ cm^{-2}}$	$\frac{Q_{PdO_x}}{405\mu C\ cm^{-2}}$
$PdCu_2$-1	24.74	22.98	34.54
$PdCu_2$-2	52.81	50.67	59.27
Pd	26.42	24.83	27.78

Table S1. Comparison of ECSA values calculated based on different electrochemical methods.

Catalysts	Atomic ratio (Pd/M)	ECSA	Mass activity
$PdCu_2$-1	1/2.11	22.98 $m^2 g^{-1}$	1290 mA mg^{-1}
$PdCu_2$-2	1/2.05	50.67 $m^2 g^{-1}$	1630 mA mg^{-1}
$Pd_{21}Cu_{79}$ [4]	1/3.76	--	1782 mA mg_{Pd}^{-1}
3D branched PdCu [5]	4/1	76.9 $m^2 g^{-1}$	--
PdCu/3DGS [31]	1/1.18	(initial) 34.9 $m^2 g^{-1}$ (activated) 65.3 $m^2 g^{-1}$	-- 1140 mA mg_{Pd}^{-1}
Pd_1Cu_1/C [48]	1.02/1	41.6 $m^2 g^{-1}$	--
PdCu/CNTs [S1] PdCuSn/CNTs [S1]	1/1.09 1/1.17/0.97	39.07 $m^2 g_{Pd}^{-1}$ 37.92 $m^2 g_{Pd}^{-1}$	639.86 mA mg_{Pd}^{-1} 872.7 mA mg_{Pd}^{-1}
PdNi/C-SC [S2]	1/1.10	38.2 $m^2 g_{Pd}^{-1}$	ca. 2370 mA mg_{Pd}^{-1}
$Pd_{83}Ni_{17}$ [22] $Pd_{72}Ni_{28}$ [22] $Pd_{53}Ni_{47}$ [22]	4.88/1 2.57/1 1.13/1	37.5 $m^2 g^{-1}$ 38.3 $m^2 g^{-1}$ 40.1 $m^2 g^{-1}$	--
Pd_1Ni_1/C [23]	3.06/1	48.1 $m^2 g_{Pd}^{-1}$	--
Pd_1Fe_1-NL/C [24]	1/1.02	50.9 $m^2 g_{Pd}^{-1}$	--
$Pd_{45}Pt_{55}$ [19]	1/1.22	--	940 mA mg_{Pd}^{-1}

Table S2. The comparison of electrochemical performance on the as-prepared $PdCu_2$ NPs modified-electrodes with other Pd-based catalysts reported in the literatures.

References

S1. Zhu, F. C., Ma, G. S., Bai, Z. C., Huang, R. Q., Tang, B., Zhang, Z. H., Wang, X. G. High Activity of Carbon Nanotubes Supported Binary and Ternary Pd-based Catalysts for Methanol, Ethanol and Formic Acid Electro-Oxidation. *J. Power Sources* **2013**, *242*, 610-620.

S2. Yang, H. J., Wang, H., Li, H., Ji, S., Davids, M. W., Wang, R. F. Effect of Stabilizers on the Synthesis of Palladium-Nickel Nanoparticles Supported on Carbon for Ethanol Oxidation in Alkaline Medium. *J. Power Sources* **2014**, *260*, 12-18.